Supplementary S1. Construction of the auxiliary information spatial database.

To compile the auxiliary information database for this study we performed an initial literature review to identify potential sources of information correlated with different factors affecting above ground biomass change, ΔAGB. We evaluated the potential of different datasets to provide information correlated to ΔAGB. We also assessed the compatibility of each dataset with the scope and needs of PNW-FIA and considered factors such as resolution, temporal and spatial coverage, interpretability, and planned updates and maintenance in the initial screening of data sources. After this revision process, we selected eight base datasets that provided the raw information used to derive the auxiliary variables that were finally included in the database. These data sources and their associated auxiliary variables were classified as:

Proxies for potential forest AGB productivity

1. 30-year climate normals for the period 1981-2010 from the Parameter-elevation Regressions on Independent Slopes Model, PRISM, developed by the Oregon State University PRISM group [1].
2. Cleland et al. [2] level-3 ecoregions (i.e., “subsections”).
3. 1 arc-second (30 m) Shuttle Radar Topography Mission, SRTM, digital terrain models

Proxies for disturbance and AGB removals.

4. Disturbance maps from the Landscape Change Monitoring System, LCMS, Science Team
5. Fire severity maps from the Monitoring Trends in Burn Severity, MTBS, program.
6. Changes in the United States National Land Cover Database, NLCD, maps.

Proxies for management regimes

7. Ownership maps maintained by the Oregon-Washington Bureau of Land Management, BLM, office.

Multitemporal AGB maps developed with data independent of FIA.

8. The multiyear forest AGB map by Fekety and Hudak [3] was developed using lidar data from 176 collections acquired between 2002 and 2016 and annual Landsat image time series (2000-2016), climate and topographic metrics

The proxies for potential forest AGB productivity were selected with the aim of obtaining information about the main intrinsic characteristics of the region that influence vegetative growth. These variables are not expected to change substantially during 2002-2018. The proxies for disturbance and land-use change provide information potentially correlated to forest AGB removals. Events mapped by auxiliary variables in this category include fires, thinning, and harvest operations or insect outbreaks. The proxies for management regimes are included in the database because management practices from different stakeholders can result in substantially different forest AGB dynamics. The last base dataset is the multi-year above-ground biomass map from [3]. This map is based on auxiliary information including lidar, Landsat imagery, climate metrics, and topographic metrics and is expected to provide precise proxy values of forest AGB for all years from 2000 to 2016. However, apart from its accuracy and precision, the most important characteristic of this dataset is that it was developed using ground measurements taken in projects outside of the PNW-FIA program. Thus, it can be considered a data source independent of the PNW-FIA sampling design.

The auxiliary information database only included the derived auxiliary variables, and to facilitate and standardize the computation of estimators that rely on pixel counts, all variables were included as raster layers with a common grid and reference system. The common grid had a resolution of 30 m and used CONUS NAD83 Albers equal-area as a reference system. The coordinates of the lower-left pixel were xmin=-2,206,050 m and ymin=2,508,420 m. A GIS layer with the boundary of the state of Oregon was downloaded from the US Census Bureau https://www2.census.gov/geo/tiger/GENZ2018/shp/cb_2018_us_state_500k.zip and was used to mask all pixels whose center fell outside the state. Steps used for the computation of each auxiliary variable are described in detail in the following subsections.

Proxies for potential forest AGB productivity

Auxiliary variables considered as proxies for potential forest AGB productivity included topographic and climatic indexes and classification of ecological regions. These variables were selected to obtain

information about the main intrinsic characteristic of the territory with an influence on vegetative growth. Available auxiliary information on soils was considered initially but discarded because the coverage of the soil surveys in the state of Oregon is not complete. The resolution and detail of these surveys is significantly coarser than the resolution of all other auxiliary information datasets used in this study. All variables in this category were considered static variables as they are not expected to change substantially during the period 2002-2018.

Topographic indexes:

A 1 arc-second Shuttle Radar Topography Mission, SRTM, digital terrain model, DTM, was obtained from the Google-Earth-Engine platform [4] and then resampled using bilinear interpolation to match the common grid and reference systems of the auxiliary information spatial database. The transformed DTM directly provided values of elevation, $ELEV$, and was used to obtain the slope, $SLOPE$, and aspect of each pixel. One categorical variable was created with elevation. This variable had 3 classes of elevation with the same areal representation in the state of Oregon. $CATELEV$. Finally, aspects were transformed to heat load, HTL, index values using Equation (S1), where the maximum potential for growth was set to the Southwest direction after [5,6].

$$HTL = 0.5 * (1 + Cos(225 - Aspect)) \quad \text{(S1)}$$

The variables $ELEV$, $SLOP$ and HTL were included in the database as static and continuous variables.

Climate auxiliary variables:

Climate auxiliary information was obtained from the Parameter-elevation Regressions on Independent Slopes Model, PRISM, developed by the Oregon State University PRISM group [1]. Grids of 800 m resolution containing 30-year normals of monthly mean precipitation, monthly mean temperature, monthly minimum temperature and monthly maximum temperature for the period 1981-2010 were obtained from https://prism.oregonstate.edu/. Thirty-year normals were used to compute Paterson's climatic productivity index, $PCPI$, as

$$PCPI = 5.3 * log((V * P * G * f)/((Tmax - Tmin) * 12)) - 7.4, \quad \text{(S2)}$$

where: V is the mean monthly temperature of the warmest month in degree Celsius; P is the mean annual precipitation in mm computed summing the mean precipitation of the 12 months of the year; $Tmax$ and $Tmin$ are, respectively, the monthly maximum temperature of the warmest month and

the monthly minimum temperature of the coldest month, both in degree Celsius; G is the length of the growing period computed from mean monthly values of precipitation and temperature using Gaussen criteria as indicated in [7] but excluding days with temperatures below 5° C in which plants are expected to have very little or no growth at all [8], (i.e., number of days a year where the mean precipitation is larger than two times the mean temperature and the mean temperature is above 5° C). Finally, f is a solar radiation factor that depends on the number of sun hours per year, $nsun$, in a given point and is calculated using Equation (S3).

$$f = \frac{2500}{nsun + 1000} \tag{S3}$$

All parameters in $PCPI$ except f were computed using the 800 m grids obtained from PRISM and then resampled to the 30 m resolution of the auxiliary information database using bilinear interpolation. The solar radiation factor f was computed by first downscaling the SRTM DTM described earlier to a 600 m resolution and then using the Area Solar Radiation tool in ESRI ArcGIS 10.6 [9] to obtain $nsun$ for each pixel. The 600 m resolution was chosen because it is slightly finer than the 800 m resolution of the other climate variables and also a multiple of the 30 m resolution of the auxiliary information grid of the auxiliary information database. The solar radiation factor f was computed from the $nsun$ grid using equation (22) and resampled to the common 30 m resolution grid using bilinear interpolation. Finally, the resulting 30 m resolution grids of V, P, G, f, $Tmax$ and $Tmin$ were used to derive a 30 m $PCPI$ grid for the entire study area. The $PCPI$ index map was assumed to collect the main climate features affecting ΔAGB caused by steady growth and was included in the database as a continuous and static variable. The $PCPI$ map was also divided into three categories (low, medium and high climate productivity) with equal area and the resulting categorical variable, $CATPCPI$, was included in the database.

Clealand's Ecoregions:

In addition to the topography and climate index described above, we considered the level-3 ecoregions (i.e. "subsections"), ECO hereafter, in [10]. Mc Nab et al. [2], describe the ecoregions as: "*relatively homogeneous physical and biological components that interact to form environments of similar productive capabilities*", thus they are potentially useful descriptors of ΔAGB resulting from natural vegetation dynamics. While climate and topography play an important role in the definition of

ecoregions, other factors such as geomorphology, lithology, or soil types are also considered [2] when defining ecoregions. Thus, ecoregions cannot be considered a variable directly derived from climate and elevation only. The auxiliary variable ECO was included in the database as a categorical and static variable.

Proxies for disturbances

Proxies for disturbances and land-use changes were selected based on their potential to provide information correlated to forest AGB removals. Events mapped by these auxiliary variables include fires, thinning, and harvest operations or insect outbreaks. We selected three sets of auxiliary variables as proxies for disturbances of different nature. These sets of maps consider disturbances occurring at different dates and they were adapted to reflect changes occurring in 10-year periods. The first dataset was fire severity which provided auxiliary information specifically related to the effects of wildland fires and was based on products from the Monitoring Trends in Burn Severity, MTBS, program. The second one was a general disturbance map generated by the Landscape Change Monitoring System, LCMS, Science Team, using LANDSAT imagery. The last set of auxiliary maps was based on the land use maps from the National Land Cover Database, NLCD.

MTBS fire severity maps:

Wildland fires cause significant forest AGB losses that can frequently exceed 200 Mg ha^{-1} in the most severely affected high biomass forest within a fire perimeter [11]. The MTBS program is a US nationwide multi-agency effort to produce consistent maps of the extent and burn severity of large wildland fires that have occurred in US since 1984 [12]. Fire perimeters and burn severity maps are produced and updated by the MTBS program. MTBS fire severity maps consider seven classes (i.e., outside-fire polygons, increased greenness, underburned-unburned, low-severity, moderate-severity, high-severity, and not-mapped) that are defined based on the differenced normalized burn ratio dNBR calculated using Landsat imagery [12].

We included maximum fire severity maps in the auxiliary information database for 10-year periods derived from the MTBS fire severity maps. We first replaced the “not-mapped” category in the original fire severity maps by applying two consecutive majority filters to the pixels in this class. Then, a resampling step was necessary to transform the original MTBS grid to the base grid of the auxiliary

information database. The resampling was done using nearest-neighbor interpolation to account for the categorical nature of the MTBS products. Finally, a second pre-processing step was necessary to summarize the yearly MTBS maps into auxiliary variables relative to 10-year periods. In this step, pixels that were not affected by fire during a 10-year period were assigned to the outside-fire category. The remaining pixels were assigned to the most severe category for the 10-year period under consideration. The resulting maps, denoted as $MAXFSEV_t$, with t indicating the first year of the period, were included in the auxiliary information database and as dynamic categorical variables.

LCMS accumulated disturbance maps:

To account for the effects of other events affecting ΔAGB, disturbance maps for 10-year periods were generated using a disturbance map generated by the LCMS Science Team for the period 1984-2017. This dataset used the grid and reference system of the auxiliary information database, so no resampling operations were necessary. The LCMS disturbance map provided the starting year, duration, and magnitude of up to 9 disturbances from 1984-2017. Disturbances were not attributed to any specific agent and their magnitudes were measured using the relativized differenced normalized burn ratio RdNBR. For every pixel in the study area, we constructed a continuous RdNBR disturbance profile using the following method. From the year 1984 to the year when the first disturbance was detected, the disturbance profile value was 0. Then the profile had a slanted segment whose width was the duration of the first disturbance. They coordinate at the end of this segment, the end of the last year of the disturbance, was the magnitude reported in the LMCS map. The profile continued with a flat segment, i.e., no change in y, until the second disturbance was found and added a new slanted segment. This process was repeated until no more disturbance events were left. Finally, the last segment of the profile was a flat segment from the end of the last disturbance to the end of year 2017 (Figure S1).

The disturbance profiles were used to calculate accumulated RdNBR disturbance values for 10-year periods. For each ten, the accumulated disturbance of a given pixel was computed from the RdNBR disturbance profile as the difference between the y coordinate of the last year of the period minus the y coordinate of the first year the period. We will refer to the auxiliary variables resulting from

accumulating disturbances in 10-year periods as $ACDIST_t$ where t represents the first year of the period. These variables were included in the database as dynamic and continuous variables.

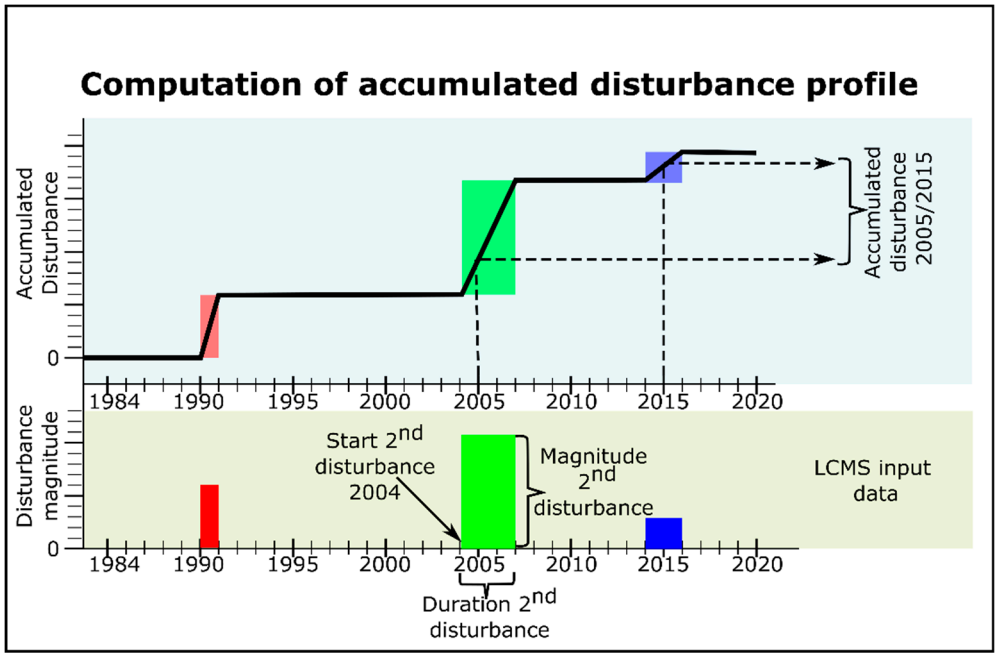

Figure S1. Construction of accumulated disturbance profile and computation of accumulated disturbance for a 10-year period using LCMS data.

Presence/absence of disturbance events

We derived an additional categorical auxiliary variable, $CATACDIST_t$, by combining $FSEV_t$ and $ACDIST_t$. This variable indicated areas suffering no disturbances, minor disturbances and major-disturbances. Pixels where $ACDIST_t$ was zero and their $FSEV_t$ class was outside-fire were assigned to the no-disturbance category. The remaining pixels were assigned to the minor or major disturbance category based on the values of $ACDIST_t$. We established a threshold to separate minor and major disturbances using pixels inside the MTBS fire polygons as reference. We obtained a sample of 282,800 pixels inside MTBS fire polygons and pixels classified as affected by moderate or high severity fire effects were assigned the value 1 and pixels in the low severity, unburned or underburned, or increased greenness categories were assigned the value 0. This subsample was used to fit a simple logistic generalized linear model with $ACDIST_t$ as predictor, instead of using a 0.5 probability to derive the threshold for classification, we used the PresenceAbsence R package [13] to search for the value of the linear predictor that optimized the Kappa index. This threshold was used to classify all pixels

that were not included in the initial no-disturbance category. The resulting maps, $CATACDIST_t$, were included in the database as dynamic and categorical variables.

NLCD land-cover change

We used the NLCD land-cover maps [14] for 2001, 2004, 2006, 2008, 2011, 2013, and 2016 to generate maps of land-cover change for 10-year periods. The NLCD land-cover maps were obtained from https://www.mrlc.gov/data and do not provide a yearly stack of land-cover maps which required defining criteria to select NLCD land-cover maps for the beginning and end of each 10-year period. That map was selected when the beginning or end of a 10-year period had an associated NLCD land-cover map. When the beginning or end of a 10-year period did not have an associated NLCD land-cover map, the NLCD map for the closest year was selected. If two NLCD maps were at the same distance from the beginning or end of the 10-year period, the NLCD map that resulted in an interval closest to 10 years was chosen. For example, for the period 2005-2015, the closest NLCD map for the end of the period is from the year 2016, but the NLCD maps for years 2004 and 2006 both have a lag of 1 year with respect to 2005. In this case, the NLCD map from 2006 was selected as the period 2006-2016 results in a 10-year difference while the NLCD map from 2004 results in a 12-year difference. NLCD land-cover maps used to derive land-cover changes for each 10-year period under consideration are reported in Table S1.

Land-cover maps from NLCD have a hierarchical legend that considers a detailed set of land-cover types. Before computing changes, we reclassified the NLCD legend into forest/non-forest by considering forest as NLCD classes 41, 42, and 43. Once NLCD maps were reclassified we calculated changes for each 10-year period. The resulting maps, $\Delta NLCD_t$, were included in the auxiliary information database as dynamic categorical variables and contained four possible values of land-cover change (Forest remains Forest, Forest to Non-Forest, Non-Forest to Forest and Non-Forest remains Non-Forest).

Table S1. NLCD maps used to derive land-cover change auxiliary maps for each 10-year period.

Period	NLCD beginning year	NLCD end year
2001-2011	2001	2011
2002-2012	2001	2011
2003-2013	2004	2013

2004-2014	2004	2013
2005-2015	2006	2016
2006-2016	2006	2016
2007-2017	2006	2016
2008-2018	2008	2016

Ownership

Management practices from different stakeholders can result in very different forest AGB dynamics. For example, in the western part of the state, the privately owned industrial forest is typically managed with short rotation periods (i.e., 40-50 years) and clear-cuts result in most of the forest AGB being removed at the end of the rotation period. This cycle is very different to the one used in some areas managed by state or federal agencies, where creating a stable and diverse forest structure is typically the priority. To account for different stakeholders' management practices, we used the land tenure zones map maintained by the Oregon-Washington Bureau of Land Management, BLM, office (https://navigator.blm.gov/api/share/pub_5c190af841654394). This map includes 26 ownership categories differentiating between different federal agencies, state and local public entities and several types of private stakeholders. The 26 original categories were reclassified into six broader groups (1 US Forest Service, 2 BLM, 3 Other federal, 4 State and local, 5 Private and tribal, and 6 Water). While ownership changes certainly occur, we considered OWN as a static categorical variable during the period 2002-2017. This is a limitation, but no ownership maps with a better temporal resolution were available. In addition, we considered extensive ownership classes that support the idea that these categories will not vary much over the period 2002-2018, as most ownership changes can be expected to occur within single ownership classes (e.g., private owners to private owners).

Change in multi-year forest AGB map

The multiyear forest AGB map by Fekety and Hudak [3] was developed using lidar data from 176 collections acquired between 2002 and 2016, Landsat imagery, climate metrics and topographic metrics as auxiliary information. A sample of 3805 field plots collected by different stakeholders [15,16] and independent of the PNW-FIA inventory was used to train random forest models to predict forest AGB. These were single-date predictions corresponding to the dates when the ground data were collected and within three years of the lidar collection date. Single-date predictions were then projected forward and backwards using Landsat time series and climate and topographic metrics to

generate forest AGB trajectories for the period 2001-2016 for each pixel. A bias correction factor was finally applied to each year's map to scale means derived from the map to totals means derived using FIA plots in the mapped area using FIA plots. To eliminate any double use of the plot data collected by FIA, we used the uncorrected predictions of AGB biomass for each year.

We used the forest AGB trajectories to generate predictions of forest ΔAGB per year for each 10-year interval under analysis. For all periods except for the decade 2007-2017 and 2008-2018 the forest ΔAGB per year was computed as difference between the forest AGB for time $t + 10$ and the forest AGB for time t divided by 10. For the decades 2007-2017 and 2008-2018, we calculated the per year change in forest AGB for 2007-2016 and 2008-2016 and divided the result by nine and eight years, respectively. This variable is a continuous variable that we denoted as ΔCMS_t. We derived an auxiliary variable for EPS estimators based on categorical variables. This variable, $CAT\Delta CMS_t$, was defined binning the range of values of ΔCMS_t with the following intervals $(-\infty, -8]$, $(-8, -4]$, $(-4, 0]$, $(0,4]$, $(4,8]$ and $(8, \infty)$. Both, ΔCMS_t and $CAT\Delta CMS_t$ were considered dynamic auxiliary variables.

References

1. PRISM Climate Group, Oregon State University Parameter-Elevation Regressions on Independent Slopes Model, PRISM, 800m Resolution 30-Year Normals 2019.
2. McNab, W.H.; Cleland, D.T.; Freeouf, J.A.; Keys, J.; Nowacki, G.; Carpenter, Ca. Description of Ecological Subregions: Sections of the Conterminous United States. *Gen. Tech. Rep. WO-76B* **2007**, *76*, 1–82.
3. Fekety, P.A.; Hudak, A.T. Annual Aboveground Biomass Maps for Forests in the Northwestern USA, 2000-2016. **2019**, doi:10.3334/ORNLDAAC/1719.
4. Gorelick, N.; Hancher, M.; Dixon, M.; Ilyushchenko, S.; Thau, D.; Moore, R. Google Earth Engine: Planetary-Scale Geospatial Analysis for Everyone. *Remote Sens. Environ.* **2017**, doi:10.1016/j.rse.2017.06.031.
5. Rodman, H. Forest Soils and Topography: Decoding the Influence of Physical Site Characteristics on Soil Water and Forest Productivity in Oregon's Coast Ranges. **2016**.
6. Stage, A.R. An Expression for the Effect of Aspect, Slope, and Habitat Type on Tree Growth. *For. Sci.* **1976**, *22*, 457–460.
7. Benavides, R.; Roig, S.; Osoro, K. Potential Productivity of Forested Areas Based on a Biophysical Model. A Case Study of a Mountainous Region in Northern Spain. *Ann. For. Sci.* **2009**, *66*, 108–108.

8. Körner, C. Treelines Will Be Understood Once the Functional Difference between a Tree and a Shrub Is. *Ambio* **2012**, *41 Suppl 3*, 197–206, doi:10.1007/s13280-012-0313-2.
9. ESRI ArcGIS Desktop: Release 10.6. Redlands, CA: Environmental Systems Research Institute. 2017.
10. Cleland, D.T.; Freeouf, J.A.; Keys, J.E.; Nowacki, G.J.; Carpenter, C.A.; McNab, W.H. Ecological Subregions: Sections and Subsections for the Conterminous United States. *Gen. Tech. Rep. WO-76D* **2007**, *76*.
11. McCarley, T.R.; Hudak, A.T.; Sparks, A.M.; Vaillant, N.M.; Meddens, A.J.H.; Trader, L.; Mauro, F.; Kreitler, J.; Boschetti, L. Estimating Wildfire Fuel Consumption with Multitemporal Airborne Laser Scanning Data and Demonstrating Linkage with MODIS-Derived Fire Radiative Energy. *Remote Sens. Environ.* **2020**, *251*, 112114, doi:10.1016/j.rse.2020.112114.
12. Picotte, J.J.; Bhattarai, K.; Howard, D.; Lecker, J.; Epting, J.; Quayle, B.; Benson, N.; Nelson, K. Changes to the Monitoring Trends in Burn Severity Program Mapping Production Procedures and Data Products. *Fire Ecol.* **2020**, *16*, 16, doi:10.1186/s42408-020-00076-y.
13. Freeman, E.A.; Moisen, G. PresenceAbsence: An R Package for Presence Absence Analysis. *J. Stat. Softw.* **2008**, *23*, 1–31.
14. Jin, S.; Homer, C.; Yang, L.; Danielson, P.; Dewitz, J.; Li, C.; Zhu, Z.; Xian, G.; Howard, D. Overall Methodology Design for the United States National Land Cover Database 2016 Products. *Remote Sens.* **2019**, *11*, doi:10.3390/rs11242971.
15. Hudak, A.T.; Fekety, P.A.; Kane, V.R.; Kennedy, R.E.; Filippelli, S.K.; Falkowski, M.J.; Tinkham, W.T.; Smith, A.M.S.; Crookston, N.L.; Domke, G.M.; et al. A Carbon Monitoring System for Mapping Regional, Annual Aboveground Biomass across the Northwestern USA. *Environ. Res. Lett.* **2020**, *15*, 095003, doi:10.1088/1748-9326/ab93f9.
16. Fekety, P.A.; Hudak, A.T.; Bright, B.C. Tree and Stand Attributes for "A Carbon Monitoring System for Mapping Regional, Annual Aboveground Biomass across the Northwestern USA". *For. Serv. Res. Data Arch.* 2020.

Supplementary S2. Summary TREE-EPS and TREE-EPS-CMS.

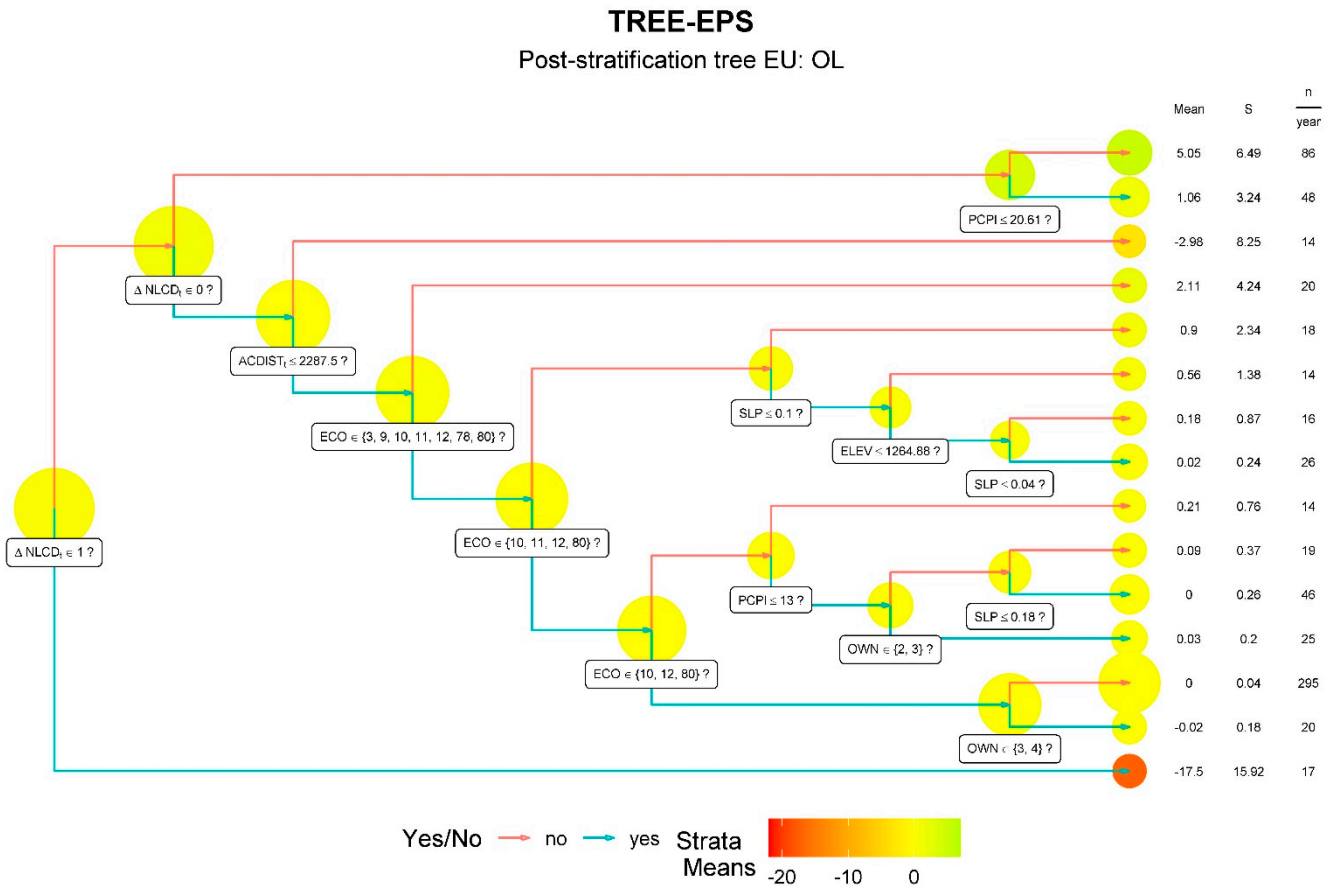

Figure S2. Partitioning tree for TREE-EPS for the estimation unit other lands (OL). Auxiliary variables are: changes in NLCD classes ($\Delta NLCD_t$), accumulated disturbance from LCMS for the period t and t +10, ($ACDIST_t$), ecoregion (ECO), Paterson climate productivity index (PCPI), ownership (OWN), slope (SLP) and elevation (ELEV). See Appendix A for details about the computation of each auxiliary variable. The size of the circles around each node of the tree is proportional to the size of the group being split.

TREE-EPS

Post-stratification tree EU: NF

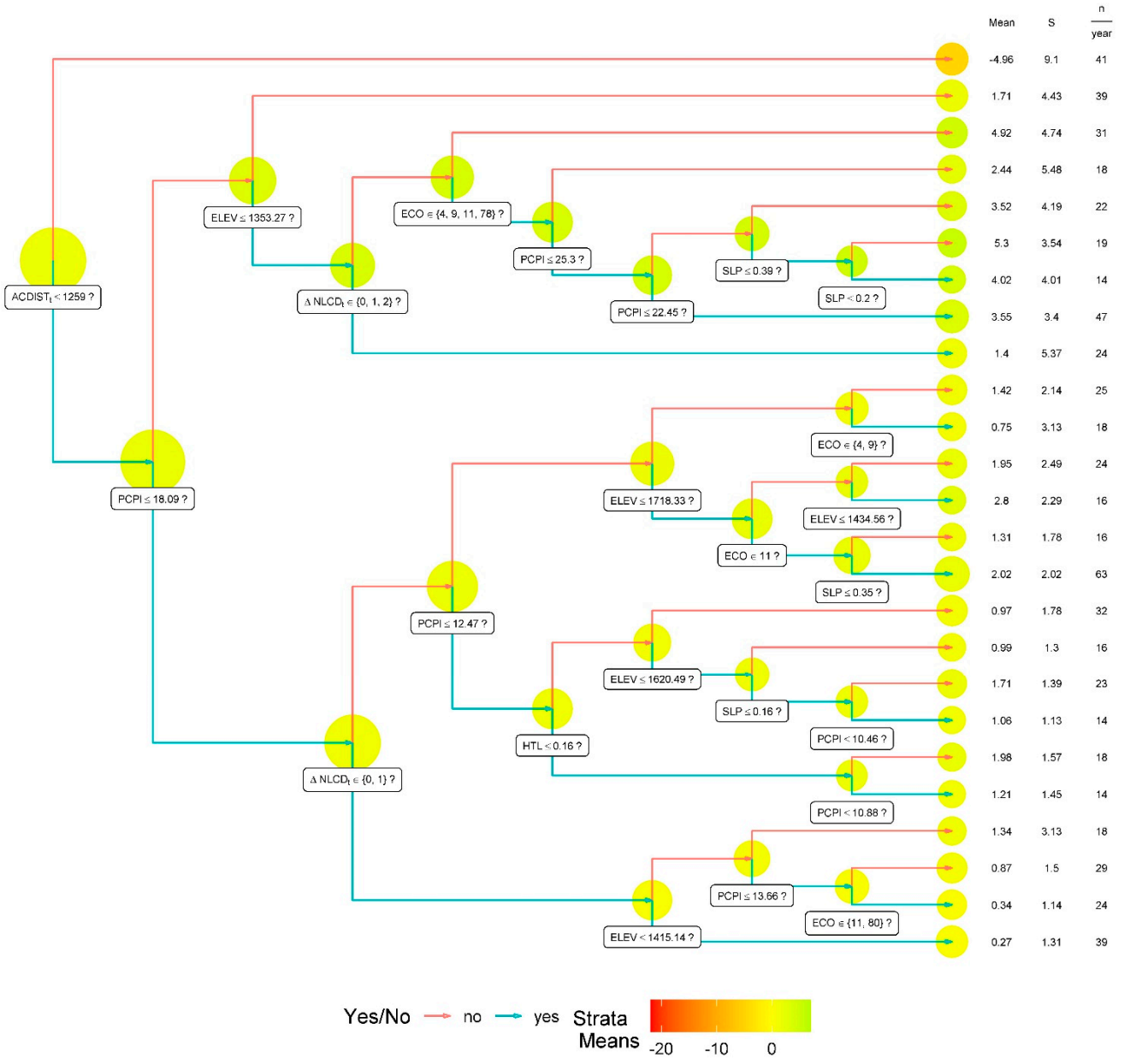

Figure S3. Partitioning tree for TREE-EPS for the estimation unit national forest lands not classified as wilderness areas (FS). Auxiliary variables are: changes in NLCD classes ($\Delta NLCD_t$), accumulated disturbance from LCMS for the period t and t +10, ($ACDIST_t$), ecoregion (ECO), Paterson climate productivity index (PCPI), ownership (OWN), slope (SLP) and elevation (ELEV). See Appendix A for details about the computation of each auxiliary variable. The size of the circles around each node of the tree is proportional to the size of the group being split.

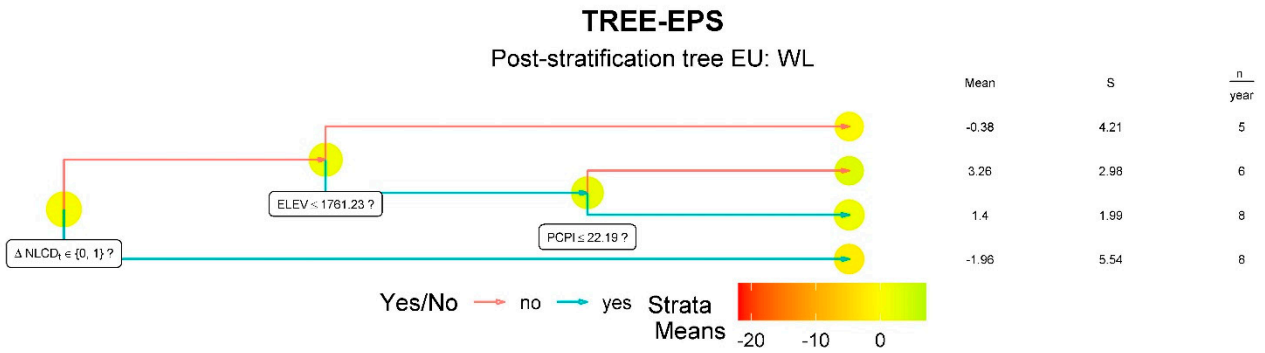

Figure S4. Partitioning tree for TREE-EPS for the estimation unit national forest lands designated as wilderness areas (WL). Auxiliary variables are: changes in NLCD classes ($\Delta NLCD_t$), accumulated disturbance from LCMS for the period t and t +10, ($ACDIST_t$), ecoregion (ECO), Paterson climate productivity index (PCPI), ownership (OWN), slope (SLP) and elevation (ELEV). See Appendix A for details about the computation of each auxiliary variable. The size of the circles around each node of the tree is proportional to the size of the group being split.

TREE-EPS-AGB

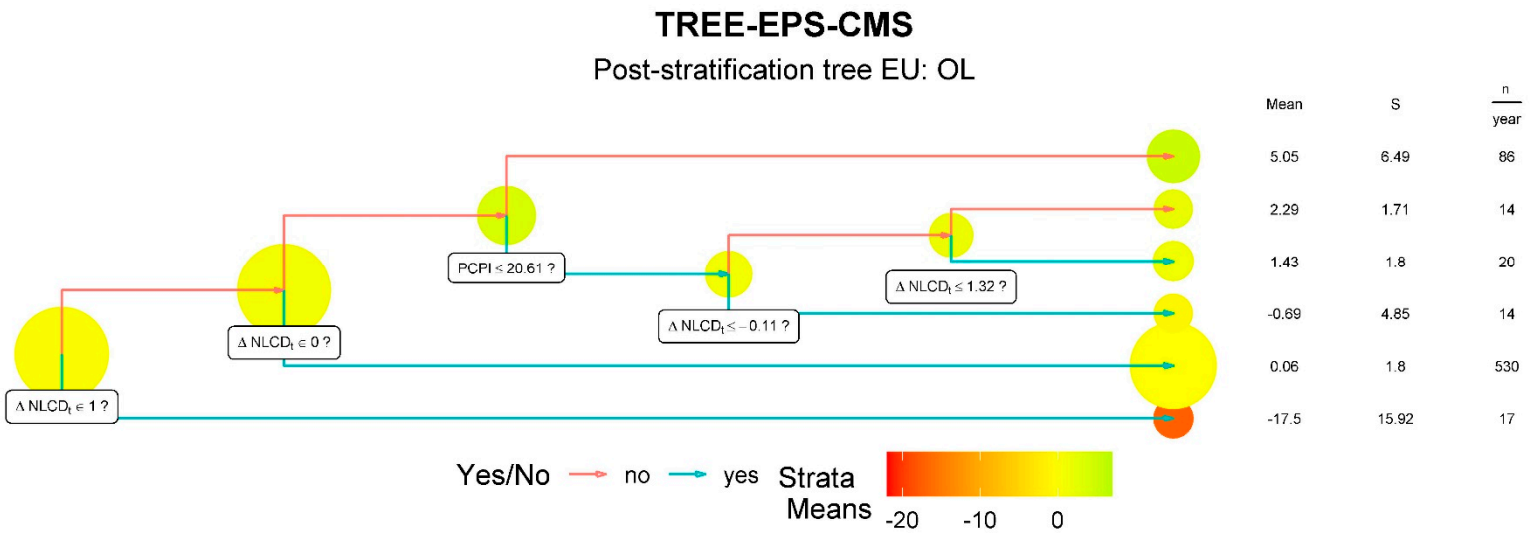

Figure S5. Partitioning tree for TREE-EPS-CMS for the estimation unit other lands (OL). Auxiliary variables are: changes in NLCD classes ($\Delta NLCD_t$), change is the difference between predictions of AGB from CMS map for years t and t +10, (ΔCMS_t), ecoregion (ECO), Paterson climate productivity index (PCPI), ownership (OWN), slope (SLP,) and elevation (ELEV). See Appendix A for details about the computation of each auxiliary variable. The size of the circles around each node of the tree is proportional to the size of the group being split.

TREE-EPS-CMS

Post-stratification tree EU: NF

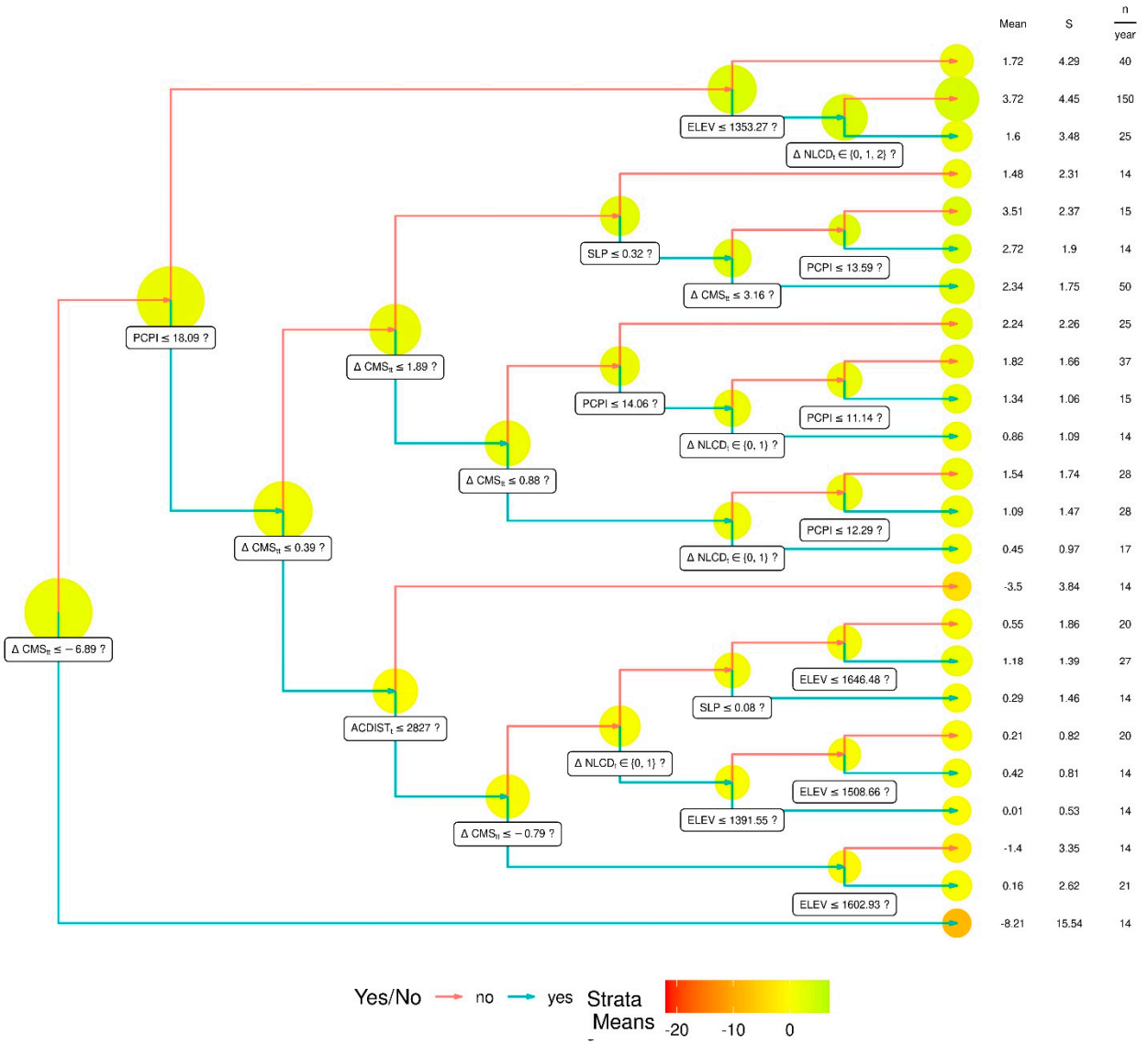

Figure S6. Partitioning tree for TREE-EPS-CMS for the estimation unit national forest lands not classified as wilderness areas (FS). Auxiliary variables are: changes in NLCD classes ($\Delta NLCD_t$), change is the difference between predictions of AGB from CMS map for years t and t +10, (ΔCMS_t), ecoregion (ECO), Paterson climate productivity index (PCPI), ownership (OWN), slope, (SLP) and elevation (ELEV). See Appendix A for details about the computation of each auxiliary variable.

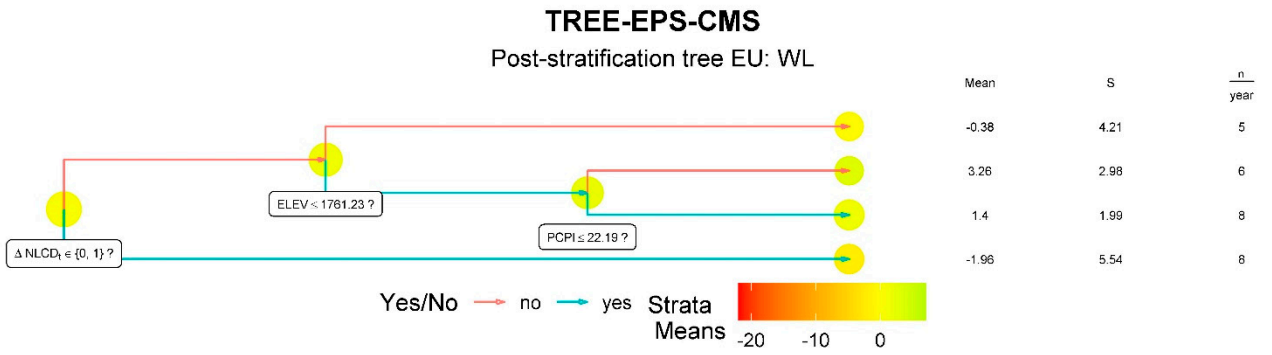

Figure S7. Partitioning tree for TREE-EPS-CMS for the estimation unit national forest lands designated as wilderness areas (WL). Auxiliary variables are: changes in NLCD classes ($\Delta NLCD_t$), change is the difference between predictions of AGB from CMS map for years t and t +10, (ΔCMS_t), ecoregion (ECO), Paterson climate productivity index (PCPI), ownership (OWN), slope (SLP) and elevation (ELEV). See Appendix A for details about the computation of each auxiliary variable. The size of the circles around each node of the tree is proportional to the size of the group being split.